

# ACAT2 and ABCG5/G8 are both required for efficient cholesterol absorption in mice: evidence from thoracic lymph duct cannulation<sup>S</sup>

Tam M. Nguyen, Janet K. Sawyer, Kathryn L. Kelley, Matthew A. Davis, Carol R. Kent, and Lawrence L. Rudel<sup>1</sup>

Department of Pathology, Wake Forest School of Medicine, Winston-Salem, NC 27157

**Abstract** The metabolic fate of newly absorbed cholesterol and phytosterol is orchestrated through adenosine triphosphate-binding cassette transporter G5 and G8 heterodimer (G5G8), and acyl CoA:cholesterol acyltransferase 2 (ACAT2). We hypothesized that intestinal G5G8 limits sterol absorption by reducing substrate availability for ACAT2 esterification and have attempted to define the roles of these two factors using gene deletion studies in mice. Male ACAT2<sup>-/-</sup>, G5G8<sup>-/-</sup>, ACAT2<sup>-/-</sup>G5G8<sup>-/-</sup> (DKO), and wild-type (WT) control mice were fed a diet with 20% of energy as palm oil and 0.2% (w/w) cholesterol. Sterol absorption efficiency was directly measured by monitoring the appearance of [<sup>3</sup>H]sitosterol and [<sup>14</sup>C]cholesterol tracers in lymph after thoracic lymph duct cannulation. The average percentage (± SEM) absorption of [<sup>14</sup>C]cholesterol after 8 h of lymph collection was 40.55 ± 0.76%, 19.41 ± 1.52%, 32.13 ± 1.60%, and 21.27 ± 1.35% for WT, ACAT2<sup>-/-</sup>, G5G8<sup>-/-</sup>, and DKO mice, respectively. [<sup>3</sup>H]sitosterol absorption was <2% in WT and ACAT2<sup>-/-</sup> mice, whereas it was up to 6.8% in G5G8<sup>-/-</sup> and DKO mice. G5G8<sup>-/-</sup> mice also produced chylomicrons with ~70% less cholesterol ester mass than WT mice. In contrast to expectations, the data demonstrated that the absence of G5G8 led to decreased intestinal cholesterol esterification and reduced cholesterol transport efficiency. Intestinal G5G8 appeared to limit the absorption of phytosterols; ACAT2 more efficiently esterified cholesterol than phytosterols. The data indicate that handling of sterols by the intestine involves both G5G8 and ACAT2 but that an additional factor (possibly Niemann-Pick C1-like 1) may be key in determining absorption efficiency.—Nguyen, T. M., J. K. Sawyer, K. L. Kelley, M. A. Davis, C. R. Kent, and L. L. Rudel. ACAT2 and ABCG5/G8 are both required for efficient cholesterol absorption in mice: evidence from thoracic lymph duct cannulation. *J. Lipid Res.* 2012. 53: 1598–1609.

**Supplementary key words** chylomicrons • cholesterol esterification • intestinal cholesterol absorption • phytosterol absorption • sitosterolemia

This work was funded by National Institutes of Health Grant HL-49373 and the Howard Hughes Medical Institute Gilliam Fellowship for Advanced Studies. Its contents are solely the responsibility of the authors and do not necessarily represent the official views of the National Institutes of Health.

Manuscript received 26 March 2012 and in revised form 24 May 2012.

Published, JLR Papers in Press, June 5, 2012  
DOI 10.1194/jlr.M026823

Beginning in 1974, the identification of sitosterolemia (1), a rare recessive disorder characterized by elevated plasma and tissue concentrations of phytosterols, has focused attention on the basic molecular processes that govern how the body normally absorbs animal-derived dietary cholesterol while excluding all other similarly structured plant-derived sterols, generally called phytosterols. Phytosterols, including campesterol, stigmasterol, and sitosterol, differ from cholesterol mainly in possessing one or two additional carbons in side chains at C24. The average North American diet contains about equal amounts of cholesterol and phytosterols (~150–400 mg/day) (2–5), yet <5% of phytosterols are absorbed compared with ~50% of cholesterol (4, 6). Thus in healthy individuals, sensitive mechanisms exist that allow the body to distinguish among modestly different sterol structures.

In general, different species of sterols have different absorption efficiencies; the closer the structural similarity to the cholesterol molecule, the higher the percentage absorption (4, 7). Even mildly hypercholesterolemic patients have serum concentrations of phytosterols that are 500 (campesterol) to 20,000 (sitosterol) times lower than that of cholesterol. Patients with sitosterolemia have increased fractional sterol absorption rates and impaired biliary secretion of neutral sterols, resulting in accumulations of these sterols in the blood and tissues (1, 8), premature atherosclerosis, and tendon/skin xanthomatosis (8, 9). Sitosterolemia has been linked to mutations in either adenosine triphosphate-binding cassette transporter G5 or G8

Abbreviations: ATF-6, activating transcription factor 6; CE, cholesterol ester; DDIT-3, DNA damage-inducible transcript 3; ER, endoplasmic reticulum; FC, free cholesterol; FP, free phytosterol; G5G8, adenosine triphosphate-binding cassette transporter G5 and G8 heterodimer; GI, gastrointestinal; MTP, microsomal triglyceride transfer protein; NPC1L1, Niemann Pick C1-like 1; PE, phytosterol ester; PL, phospholipid; SI, small intestine; TG, triglyceride; TLD, thoracic lymph duct; TLDC, TLD cannulation; WT, wild-type; XBP-1, X-box binding protein 1; XBP-1p, X-box binding protein 1 spliced variant.

<sup>1</sup>To whom correspondence should be addressed.

e-mail: lrudel@wakehealth.edu

<sup>S</sup>The online version of this article (available at <http://www.jlr.org>) contains supplementary data in the form of two figures and one table.

Copyright © 2012 by the American Society for Biochemistry and Molecular Biology, Inc.

This article is available online at <http://www.jlr.org>

(ABCG5 or ABCG8), which are expressed almost exclusively in hepatocytes and enterocytes forming a heterodimer (G5G8) typically localized to the plasma membrane (10, 11). Another protein that is expressed exclusively in the same two cell types is acyl CoA:cholesterol acyltransferase type 2 (ACAT2), a cholesterol-esterifying enzyme residing in the endoplasmic reticulum (ER) membrane (12).

Mice lacking G5G8 have phenotypes resembling patients with sitosterolemia, including increased fractional absorption of noncholesterol sterols, marked accumulation of sitosterol and campesterol in the blood and liver, reduced levels of biliary cholesterol, and various hemolytic disorders (7, 13). These findings suggested that the physiological role of G5G8 is to limit phytosterol accumulation in the body by limiting its absorption in the intestine and by promoting its secretion from the liver. Because sitosterolemic patients and G5G8 knockout (G5G8<sup>-/-</sup>) mice can still maintain the same rank order of absorption efficiency (cholesterol > campesterol > sitosterol), it has been suggested that other proteins independent of G5G8 are responsible for the selectivity of cholesterol over phytosterol absorption (13, 14).

In the enterocyte, the esterification of a free cholesterol (FC) molecule with a fatty acid from acyl-CoA to synthesize a cholesterol ester (CE) molecule changes the physicochemical state of cholesterol from a relatively membrane-soluble lipid into a more insoluble CE molecule that must be packaged into the neutral lipid core of chylomicron particles for transport (15). Chylomicrons are secreted directly into the lymphatic system where they pool in the cisternae chyli, travel up the thoracic lymph duct, and enter the circulatory system at the subclavian vein (15, 16). Although the cross-talk between G5G8 and ACAT2 is unknown, it is possible that, together, the relative functions of G5G8 and ACAT2 in the enterocyte dictate the fate of newly absorbed cholesterol and phytosterols as they traverse the enterocyte from the gut lumen.

The majority (70–92%) of the sterols exported into thoracic duct lymph of various animals, including rats, rabbits, monkeys, and humans, are esterified (15–19). More particularly, the percentage esterification of absorbed cholesterol is constant regardless of the extent of absorption (19). Lee et al. (12) showed that ACAT2, but not ACAT1, is exclusively expressed in hepatocytes and enterocytes. Buhman et al. (20) reported that the loss of ACAT2 activity in the intestine leads to a decrease in cholesterol absorption efficiency despite unchanged cholesterol synthesis.

To date, the degree to which ACAT2 handles cholesterol differently than phytosterols remains unclear. In vitro studies using CaCo-2 cells and rabbit intestinal microsomes have concluded that membrane sitosterol does not interfere or compete with cholesterol for esterification, and it does not alter intracellular cholesterol trafficking or CE secretion (21, 22). On the contrary, experiments performed using microsomes isolated from Chinese hamster ovary cells overexpressing either ACAT1 or ACAT2 showed that ACAT2 displayed a greater capacity to differentiate cholesterol from sitosterol, with a preference for esterifying cholesterol over sitosterol (23). These conflicting reports

led us to question what actually happens in animal models in vivo.

We hypothesized that sterols enter the enterocyte through the brush border membrane via a Niemann-Pick C1-like 1 (NPC1L1)-mediated process but that G5G8 can limit the substrate availability for ACAT2 esterification by subsequently excreting newly absorbed phytosterols and cholesterol out of the cell, in the process possibly decreasing the overall absorption efficiency of both sterols. In addition, sterol esterification by ACAT2 may enhance absorption efficiency by generating sterol esters that get packaged into chylomicron particles for secretion into lymph and, in the process, become unavailable to G5G8.

In this study, we investigated the relative contributions of G5G8 and ACAT2 in intestinal cholesterol absorption compared and contrasted with phytosterol absorption. Using the thoracic lymph duct cannulation (TLDC) technique, which allows for quantitative collection of newly absorbed sterols after a meal and characterization of chylomicron particles, this study directly addressed the following question: How does the absence of G5G8 affect cholesterol esterification and absorption efficiency during sterol metabolism in enterocytes of physiologically intact mice?

## MATERIALS AND METHODS

### Animals and diets

All mice used in these studies were housed in the animal facility at the Wake Forest School of Medicine (WFSM), which is approved by the American Association for Accreditation of Laboratory Animal Care; the Institutional Animal Care and Use Committee approved all protocols prior to execution. Male wild-type (WT), ACAT2<sup>-/-</sup>, G5G8<sup>-/-</sup>, and ACAT2<sup>-/-</sup>G5G8<sup>-/-</sup> (DKO) mice were colony mates with an identical mixed background (81.25% C57BL/6, 12.5% 129SvJae, 6.25% 129SvEv). ACAT2-deficient mice were originally generated by Buhman et al. (20), using targeted deletion of a portion of the *Soat2* gene to remove the carboxy-terminal 28% of the ACAT2 protein. G5G8-deficient mice were generated as described by Yu et al. (24). Briefly, the murine *Abcg5* and *Abcg8* genes, similar to the human genes, are located in a head-to-head position within 400 bp of each other. To generate mice that were homozygous for disrupted *Abcg5* and *Abcg8* allele, the region spanning intron 2 of *Abcg5* and intron 3 of *Abcg8* was deleted, rendering dysfunctional proteins without the Walker A sequences at the ATP-binding site. Mice used in this study were the offspring of matings between mice heterozygous for disrupted *Abcg5* and *Abcg8* alleles and mice heterozygous for a disrupted *Soat2* allele. Mice were maintained on a rodent chow diet until 11–12 weeks of age, when feeding was begun with a semisynthetic saturated fat diet (sat. diet) containing 20% of energy as palm oil and 0.2% (wt/wt) cholesterol for five weeks. This diet was chosen because it is relatively low in plant sterol and more representative of a human-like diet than chow. In one study, mice (n = 9–10 mice/genotype) underwent TLDC surgery for direct measurement of sterol absorption from a meal using radioactive tracers, followed by plasma and tissue collection. In another study, a baseline blood sample was taken from mice (n = 7–8/genotype) prior to study initiation, the sat. diet was then fed for five weeks and an additional blood sample was taken, a three-day fecal sample was collected for measurement of fecal neutral sterol excretion (25), and finally, tissues were harvested after euthanasia

and were snap-frozen in liquid nitrogen and stored at  $-80^{\circ}$  until analysis.

### Cholesterol absorption measurement by thoracic lymph duct cannulation (TLDC)

Using a modified version of the surgical procedures previously described by Ionac (26), the thoracic lymph ducts (TLD) of mice (9–10/genotype) were cannulated. The procedure was performed as previously described (27).

In brief, mice were gavaged with 25  $\mu$ l soybean oil 30 min prior to surgery to facilitate visualization of the lymphatic vessels. Ketoprofen (5 mg/kg body weight) was injected subcutaneously as an analgesic. Mice were anesthetized with isoflurane (4% for induction, 2–3% for maintenance) during surgery. The proximal duodenum was cannulated approximately 5 mm below the pyloric sphincter through the stomach. A mixed micelle solution (3 mM egg lecithin, 16 mM oleic acid, and 54 mM NaTC in complete PBS) was constantly infused into the duodenum via the cannula at a rate of 300  $\mu$ l per h using a syringe pump (Harvard Apparatus) for the duration of the experiment. The complete PBS contained 6.75 mM  $\text{Na}_2\text{HPO}_4$ , 16.5 mM  $\text{NaH}_2\text{PO}_4$ , 115 mM NaCl, 15 mM KCl, 10 mM glucose, and 1 mM  $\text{CaCl}_2$  at pH 6.4 (Sigma). To begin the experiment, a bolus dose of radioactive micelle solution (6  $\mu$ Ci [ $^3\text{H}$ ] $\beta$ -sitosterol and 2  $\mu$ Ci [ $^{14}\text{C}$ ]cholesterol, 3.8 mM cholesterol, 0.7 mM sitosterol, 35.2 mM egg lecithin, 200 mM NaTC in complete PBS) was injected directly into the duodenum below the pyloric sphincter. Then, the TLD cannula was inserted into the TLD above the cisterna chyli between the transverse lumbar artery and the diaphragm. The time lapse between administration of the radioactive micelle dose and thoracic lymph drainage varied between 5 and 10 min. Upon establishment of lymph flow, the abdomen was closed, and isoflurane anesthesia was removed. Mice were immediately restrained on an exercise wheel in a conscious state to allow free body movement. Lymph was drained into a tube containing 5  $\mu$ l protease inhibitor cocktail (Sigma) plus 5% EDTA and 5% sodium azide for 8 hourly collections. Percentage sterol absorption was quantitatively assessed in each animal during active lipid absorption by measuring the dpm of [ $^{14}\text{C}$ ]cholesterol and [ $^3\text{H}$ ]sitosterol in an aliquot of whole lymph from each hourly collection and then dividing by the total dpm in the bolus dose injected into the duodenum. The absorption efficiency of each individual animal was calculated as the cumulative percentage of radioactive dose in thoracic duct lymph by the end of 8 h.

### Chylomicron isolation and particle composition analyses

Chylomicrons were isolated by ultracentrifugation of whole lymph, and chylomicron particle analyses were performed as described previously (27). The chylomicron diameter ( $n = 9\text{--}10/\text{genotype}$ ) was measured by dynamic light scattering using the Zetasizer Nano (Malvern Instruments), following the manufacturer's instructions. Chylomicrons isolated from the hours 3 and 4 collections were used because these fractions corresponded with the peak times of cholesterol absorption during the 8 h time course. Chylomicron size from the hours 7 and 8 collections was also measured; no statistically significant differences were found between Z-averages of either measurement set.

### Plasma lipid analyses

Plasma cholesterol concentrations were analyzed while the mice were on rodent chow and again after 5 weeks of sat. diet feeding. After a 4 h fasting period, blood was collected by superficial submandibular vein puncture, and total plasma sterol concentrations were measured using colorimetric assay as described previously (25). Concentrations of plasma cholesterol and

phytosterols (including campesterol, stigmasterol, and sitosterol) were measured using gas liquid chromatography (GLC) according to previously published methods (28).

### Liver and jejunum mRNA expression by real-time PCR

Separate groups of mice that were not cannulated were euthanized for tissue harvest. Mice ( $n = 7\text{--}11/\text{genotype}$ ) were fasted for 4 h then anesthetized with 2  $\mu$ g/g body weight of 50 mg/ml ketamine 10 mg/ml xylazine solution by intramuscular injection. After the entire circulatory system was flushed with ice-cold saline, the small intestine (SI) was flattened on an ice-cold glass plate and cut into five segments of equal length (SI-1 to SI-5). The lumen of each segment was then flushed clean with cold saline. SI-2 and SI-3 (representing the jejunum) and the liver were snap-frozen in liquid nitrogen. Liver and jejunum mRNA expression analyses were performed as described (28). Ct values were calculated based on fluorescence measurements and entered into an equation (arbitrary unit =  $1 \times 10^9 \times e^{(0.6931 \times \text{Ct})}$ ) to determine arbitrary units (AU). All results were normalized to mRNA expression of cyclophilin as the housekeeping gene within the same sample.

### Microsomal ACAT enzyme activity assay for intestine and liver tissues

Frozen jejunum (combined segments 2 and 3) and 200–300 mg of frozen liver ( $n = 5/\text{genotype}$ ) were crushed using a mortar and pestle chilled in liquid nitrogen to prevent tissue thawing. Crushed tissue was homogenized in ACAT homogenization buffer in the presence of protease inhibitor cocktail (20  $\mu$ l for SI, 10  $\mu$ l for liver; Sigma). The microsomes were isolated, and the ACAT assays were performed as described (29) in the absence and presence of pyripyropene A (PPPA), an ACAT2-specific inhibitor, so that ACAT2 activity could be calculated. Relative ACAT enzyme activity was expressed as nanomole [ $^{14}\text{C}$ ]CE synthesized per milligram microsomal protein per minute (nmol/mg/min).

### Jejunal mucosa and hepatic lipid analyses

Mice from each genotype were euthanized as described above. The intestinal mucosa of SI-2 and SI-3 were removed by scraping gently with glass slides and then were extracted immediately with chloroform:methanol (2:1). For liver lipid composition, about 60–100 mg of liver was processed as previously described (25, 30), with the final cholesterol and phytosterol concentrations being analyzed by gas chromatography (GC) (28). The difference in total sterol mass and free sterol mass was multiplied by 1.67 to calculate sterol ester mass. All sterol concentrations were normalized to the protein concentration in the same tissue sample. To measure tissue protein mass, the delipidated tissue residue was digested in 1N NaOH and analyzed by Lowry assay (31).

### Statistical analyses

Using GraphPad Prism statistical software v4 (GraphPad Software Inc.), the data were analyzed by one-way ANOVA with Tukey posthoc tests or two-way ANOVA with Bonferroni posthoc tests. Statistically significant differences were considered at  $P < 0.05$  and are indicated by different superscript letters.

## RESULTS

TLDC was used to directly measure [ $^{14}\text{C}$ ]cholesterol absorption in the mice ( $n = 9\text{--}10/\text{genotype}$ ) with ACAT2 and G5G8 deletions (**Fig. 1A**). ACAT2 deletion was found to decrease the cumulative rate of [ $^{14}\text{C}$ ]cholesterol absorption by about 50% at all time points throughout the study;



a similar decrease was also seen when G5G8 was deleted together with ACAT2 in the DKO mice. Interestingly, the deletion of G5G8 alone resulted in a smaller but statistically significant 21% decrease in [<sup>14</sup>C]cholesterol absorption compared with that in WT mice, which was opposite of what was expected and was not additive to the decrease seen with ACAT2 deletion. Given that G5G8<sup>-/-</sup> mice have altered sitosterol absorption, fecal dual-isotope measurements (involving fecal [<sup>3</sup>H]sitosterol and [<sup>14</sup>C]cholesterol tracers to estimate fractional cholesterol absorption) were not attempted in this study. Nevertheless, we have found excellent agreement between the percentage of cholesterol absorption obtained by TLDC, as done here, and the values derived from fecal dual-isotope method in mice with intact G5G8 [in the presence or absence of ACAT2] (27). Individual animal plots of cholesterol absorption efficiency (n = 9–10/genotype) at hour 8 of the experiment show limited scatter among individual mice within each genotype (Fig. 1B); accordingly, all differences between WT and ACAT2<sup>-/-</sup>, G5G8<sup>-/-</sup>, or DKO mice were found to be statistically significant. The average values (± SEM) for the absorption of [<sup>14</sup>C]cholesterol at 8 h were 40.55 ± 0.76%, 19.41 ± 1.52%, 32.13 ± 1.60%, and 21.27 ± 1.35% for WT, ACAT2<sup>-/-</sup>, G5G8<sup>-/-</sup>, and DKO mice, respectively.

The recovery of cholesterol in the feces of ACAT2<sup>-/-</sup> mice was higher than in WT mice (Fig. 1C). Fig. 1C shows fecal recovery of cholesterol mass in separate groups of

mice (n = 7–8/genotype) that had not been cannulated. These data appeared to reflect the expected complimentary outcome to the decreased percentage cholesterol absorption in ACAT2<sup>-/-</sup> mice as seen in Fig. 1A, B. However, the recovery of cholesterol in the feces of G5G8<sup>-/-</sup> and DKO mice was lower than would be predicted from the percentage absorption outcome. This finding has been reproduced in a separate experiment and suggests that other factors in addition to the cholesterol absorption (measured directly in Fig. 1A, B) come into play. The lower fecal cholesterol excretion in G5G8<sup>-/-</sup> mice (Fig. 1C) may be attributable to decreased hepatobiliary cholesterol secretion when G5G8 is absent, which is consistent with published reports (32). With G5G8 deletion, sterols accumulate in the liver, as indicated by dramatic increases in hepatic CE, free phytosterol (FP), and phytosterol ester (PE) concentrations in G5G8-deficient mice (supplemental Fig. II-B–D). Because fecal neutral sterol content is critically dependent on biliary sterol secretion (33), it is conceivable that G5G8-deficient mice did not effectively secrete sterols into bile and therefore had lower fecal neutral sterol levels than WT mice did. An additional pathway for excretion of sterols is the transintestinal cholesterol excretion pathway, and it may also be defective in mice without the ABCG5/G8 transporter (34). A clear explanation for this discrepancy is yet to be determined.

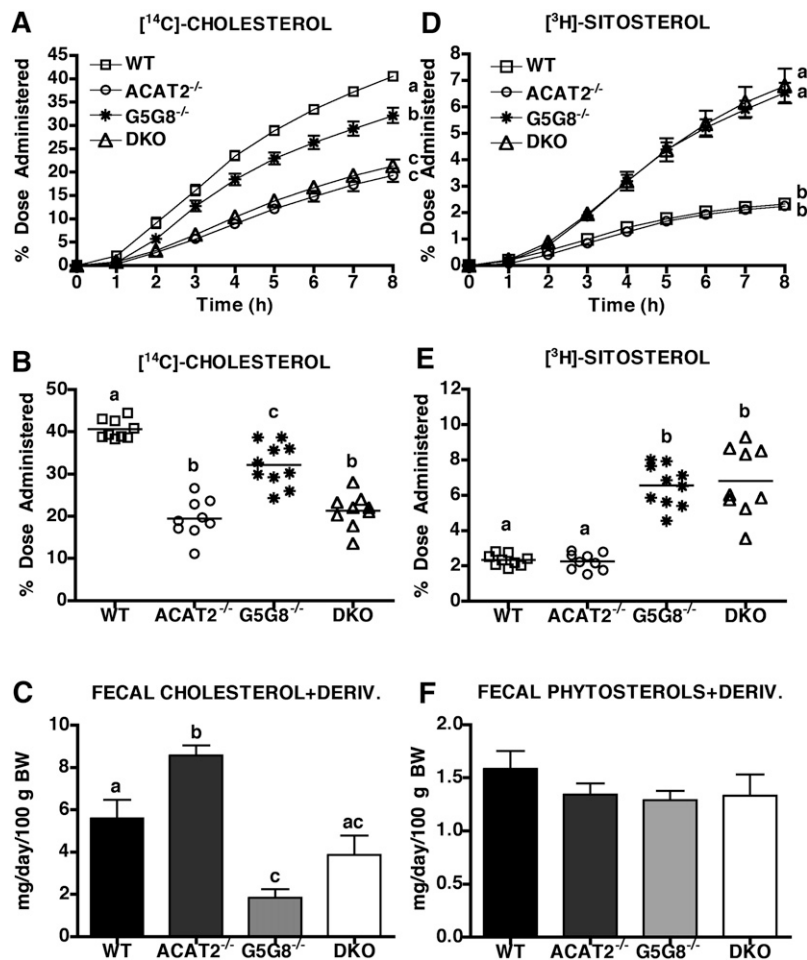


**Fig. 1.** Sterol absorption efficiency and fecal neutral sterol excretion. (A) Direct assessment of percentage cholesterol absorption efficiency by thoracic lymph duct cannulation was reported as cumulative percentage of [<sup>14</sup>C]cholesterol dose appearance in lymph over 8 hourly collections. The data represent mean ± SEM, n = 9–10/genotype. These data were analyzed by two-way ANOVA with Bonferroni posthoc test. Unlike letters designate statistically significant differences of *P* < 0.05 at the hour 8 time point. (B) Individual animal data for percentage of total [<sup>14</sup>C]cholesterol dose recovered in lymph after 8 h lymph collection. Lines represent the means, n = 9–10/genotype. (C) Fecal cholesterol and cholesterol derivatives measured in lipid extracts of dried, crushed feces from three-day collection. The data represent mean ± SEM, n = 7–8/genotype. These data were analyzed by one-way ANOVA with Tukey posthoc tests. Unlike letters indicate statistically significant differences of *P* < 0.05. (D and E) Data were obtained and analyzed as described for panels A and B with the use of [<sup>3</sup>H]sitosterol to represent phytosterol absorption. (F) Fecal phytosterols and phytosterol derivatives analyzed as described in panel C.

The efficiency of phytosterol absorption was also documented in these studies as [ $^3\text{H}$ ]sitosterol was given in the bolus dose. The cumulative absorption of [ $^3\text{H}$ ]sitosterol was much lower than cholesterol in WT and ACAT2 $^{-/-}$  mice (only reaching just over 2% at 8 h), whereas G5G8 $^{-/-}$  and DKO mice displayed significantly higher rates of [ $^3\text{H}$ ]sitosterol accumulation reaching 6.8% (Fig. 1D). The differences in cumulative appearance rates were present throughout the experiment (Fig. 1D) and also appeared in percentage absorption of [ $^3\text{H}$ ]sitosterol for individual animals at 8 h of lymph collection (Fig. 1E). The average ( $\pm$  SEM) percentages at 8 h were  $2.33 \pm 0.11\%$ ,  $2.25 \pm 0.16\%$ ,  $6.54 \pm 0.37\%$ , and  $6.79 \pm 0.65\%$  for WT, ACAT2 $^{-/-}$ , G5G8 $^{-/-}$ , and DKO mice, respectively (Fig. 1E). The significantly higher percentage of sitosterol absorption in G5G8-deficient mice was consistent with outcomes predicted in the literature (1, 7, 24, 32). Fecal phytosterol excretion (Fig. 1F) was equally low ( $\sim 1.5$  mg/day/100 g body weight) across all genotypes and did not indicate the anticipated decrease of phytosterol excretion in G5G8-deficient mice. One would expect that mice lacking the G5G8 inside-out sterol transporter would absorb more phytosterol and excrete less phytosterol into feces than those with functional G5G8. Our data did not reflect this expectation. This may have been related to the fact that phytosterols made up only a small portion of the total sterols in the gut lumen, given that the sat. diet contained significantly less phytosterol than cholesterol (1:7 w/w ratio). But with limited mass combined with the very limited efficiency of plant sterol absorption among all groups, any differences will be hard to detect.

After 8 h of lymph collection, the mice were euthanized, and the distributions of the remaining radioactive [ $^{14}\text{C}$ ]cholesterol and [ $^3\text{H}$ ]sitosterol were assessed in the intestinal wall plus luminal content of the stomach, in five consecutive segments of the small intestine, in the cecum and the colon, as well as in the liver (Fig. 2). In data not shown, we observed a similar radioactive sterol distribution pattern when we analyzed data from the walls of SI-1 to SI-5 without the luminal content. Less than 1% of the radioactive dose was found in the plasma in all mice (data not shown), confirming that the TLDC provided quantitative lymph collections. Furthermore, very little [ $^{14}\text{C}$ ]cholesterol ( $<3\%$ ) was present in plasma and liver together, suggesting that cholesterol entry into the blood via intestine-derived HDL particles is quite limited with the thoracic lymph duct fistula.

[ $^{14}\text{C}$ ]cholesterol recovered in the wall and luminal content of the GI tract revealed a distinct pattern from that of [ $^3\text{H}$ ]sitosterol (Fig. 2). The bolus dose was injected intraduodenally, and no radioactive cholesterol was detected in the stomach. [ $^{14}\text{C}$ ]cholesterol was distributed throughout the SI with the highest proportion found in SI-2 and SI-3 (the jejunum). Within each segment of the intestine, there was 2- to 3-fold more [ $^{14}\text{C}$ ]cholesterol in ACAT2 $^{-/-}$ , G5G8 $^{-/-}$ , and DKO mice compared with WT mice, with this difference reaching statistical significance in many cases. The absence of G5G8 in the proximal SI did not appear to result in more [ $^{14}\text{C}$ ]

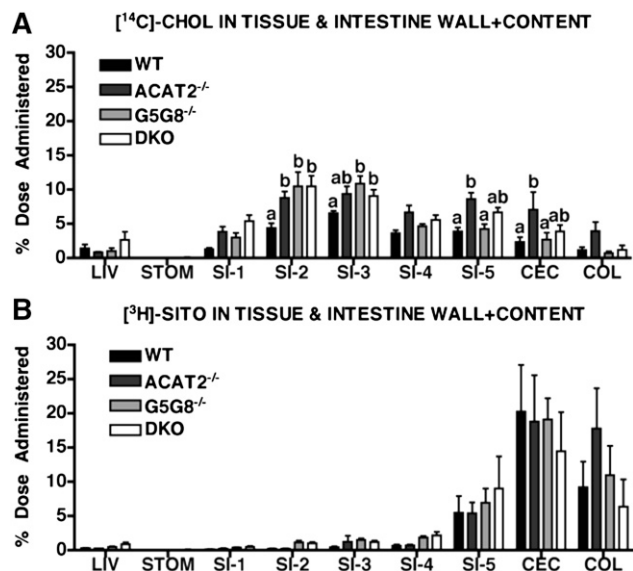


**Fig. 2.** Radioactivity recovery in the liver and gastrointestinal tract (tissue wall and lumen content) after thoracic lymph duct cannulation. After the 8 h experiment, [ $^{14}\text{C}$ ]cholesterol (A) and [ $^3\text{H}$ ]sitosterol (B) were quantified in the liver (LIV), stomach (STOM), five equal-length segments of the small intestine (SI-1 to SI-5), cecum (CEC), and colon (COL). The data are expressed as percentage of the radioactive dose administered during thoracic lymph duct cannulation surgery and represent mean  $\pm$  SEM,  $n = 5$ /genotype. Unlike letters indicate statistically significant differences ( $P < 0.05$ ) within the same tissue as determined by two-way ANOVA analyses and Bonferroni posthoc tests.

cholesterol accumulating in the SI beyond levels found in mice lacking ACAT2. In all genotypes, very little [ $^{14}\text{C}$ ]cholesterol was found in the cecum and colon, although somewhat more (up to  $\sim 10\%$ ) was found in these locations in ACAT2 $^{-/-}$  mice.

The [ $^3\text{H}$ ]sitosterol distribution pattern (Fig. 2B) along the length of the intestine was strikingly different from that observed for [ $^{14}\text{C}$ ]cholesterol (Fig. 2A). Less than 2% of the remaining [ $^3\text{H}$ ]sitosterol dose was found in each SI segment of SI-1 through SI-4, whereas more of the [ $^3\text{H}$ ]sitosterol was found in the distal portion of the GI tract in the terminal ileum (SI-5), cecum, and colon, with no statistically significant differences among all four genotypes. The data clearly show that G5G8-deficiency did not lead to the accumulation of [ $^3\text{H}$ ]sitosterol in the SI. This pattern held true whether the data was analyzed for radioactive sitosterol in the whole SI segments, as shown here, or in only WT SI wall alone (data not shown). To our knowledge, this study is the first to demonstrate the dramatic differential handling of [ $^{14}\text{C}$ ]cholesterol versus [ $^3\text{H}$ ]sitosterol down the length of the GI tract, and the data strongly suggest that separate processing occurs for these two sterols. [ $^{14}\text{C}$ ]cholesterol appeared to exchange among membranes and label the many pools of cholesterol in the gut, whereas [ $^3\text{H}$ ]sitosterol did not participate in this behavior. The possibility exists that during absorption, the [ $^3\text{H}$ ]sitosterol never efficiently gets into the intracellular membranes of the enterocyte even when G5G8 is absent, perhaps due to selection against uptake by a factor such as NPC1L1.

To further understand how the SI handles sterols, we used separate groups of mice that had not been cannulated to *i*) analyze sterol concentrations in SI mucosa of the jejunum (Fig. 3), *ii*) evaluate the mRNA expression of various genes in the jejunum (Fig. 4A, B and supplemental Table I), and *iii*) measure ACAT1 versus ACAT2 enzyme activity in the jejunum (Fig. 4C, D).

Sterol concentrations were expressed as average ( $\pm$  SEM) micrograms sterol per milligrams protein in SI mucosa from SI-2 and SI-3 combined. FC was roughly 25% higher in ACAT2<sup>-/-</sup> and DKO mice (64.8  $\pm$  6.5 and 62.1  $\pm$  3.8  $\mu$ g/mg, respectively) than in WT and G5G8<sup>-/-</sup> mice (51.3  $\pm$  2.8 and 45.2  $\pm$  2.7  $\mu$ g/mg, respectively) (Fig. 3A). ACAT2 deficiency with or without G5G8 resulted in higher FC accumulations in the SI mucosa, whereas G5G8 deficiency alone did not alter FC concentration. On the other hand, CE concentrations were lower when both ACAT2 and G5G8 were deleted (Fig. 3B). Compared with CE in mucosa of WT mice (18.8  $\pm$  2.0  $\mu$ g/mg), there was about 40% less CE in SI mucosa from ACAT2<sup>-/-</sup>, G5G8<sup>-/-</sup>, and DKO mice (12.8  $\pm$  2.2, 11.5  $\pm$  1.1, and 11.1  $\pm$  2.5  $\mu$ g/mg, respectively). The relative FC and CE mass in the SI mucosa of ACAT2<sup>-/-</sup> mice compared with WT mice were consistent with those reported by Turley et al. (35). Interestingly, FC existed in higher concentrations in the SI mucosa than CE even when ACAT2 was present, a pattern quite different from that found in the liver (supplemental Fig. II-A, B). There were dramatically higher concentrations of CE in the liver (supplemental Fig. II-B) than in the SI mucosa (Fig. 3B). WT mice had about 10-fold higher CE in the liver than in the SI mucosa, and this value was about 30-fold higher in G5G8<sup>-/-</sup> liver than in G5G8<sup>-/-</sup> SI mucosa. CE appeared to accumulate in the livers of G5G8<sup>-/-</sup> mice but did not accumulate in the SI mucosa, suggesting that the impact of G5G8 on hepatic cholesterol metabolism is different from that in the SI.

We also measured phytosterol concentrations in the SI mucosa across all four genotypes (Fig. 3C, D). Phytosterols only accumulated in the SI mucosa of mice lacking G5G8.

FP concentrations were equivalently low ( $\sim$ 1  $\mu$ g/mg protein) in SI mucosa of mice with intact G5G8 (Fig. 3C) but were almost 6-fold higher in G5G8<sup>-/-</sup> mice (5.7  $\pm$  0.4  $\mu$ g/mg protein). The deletion of ACAT2 in addition to G5G8 in the DKO mice significantly attenuated this elevation to 3.9  $\pm$  0.2  $\mu$ g/mg protein. Even though PE concentrations were >50% lower than FP, a similar trend by genotype existed. WT and ACAT2<sup>-/-</sup> mice had minimal PE (0.2  $\pm$  0.1 and 0.5  $\pm$  0.1  $\mu$ g/mg protein, respectively) in the SI mucosa, but G5G8<sup>-/-</sup> mice had 2.5  $\pm$  0.5  $\mu$ g/mg protein, and DKO had significantly less (1.0  $\pm$  0.3  $\mu$ g/mg protein). Sterol mass data of the SI mucosa suggest that some phytosterols accumulate in the enterocyte in the absence of G5G8, although it does not appear that the source is from the intestinal lumen (Fig. 2). The lack of [<sup>3</sup>H]sitosterol labeling suggests that any accumulated phytosterol mass may be derived from the liver via the blood.

In agreement with Turley et al. (35), ABCG5 mRNA was slightly elevated in ACAT2<sup>-/-</sup> mice relative to WT mice (Fig. 4B). Diminished ABCG5 mRNA expression in G5G8<sup>-/-</sup> and DKO mice is shown in Fig. 4B, where the small amount of ABCG5 message detected was most likely due to amplification of a downstream start codon forming a nonfunctional mRNA fragment. To evaluate G5G8 function, we measured plasma phytosterol concentrations in mice lacking G5G8 (supplemental Fig. I-E, F). Although plasma cholesterol concentrations were comparable among genotypes (supplemental Fig. I-C, D), a highly significant enrichment of phytosterol concentrations in the plasma of G5G8-deficient mice was found (supplemental Fig. I-E, F), clearly indicating that G5G8 was dysfunctional. On the basis of the significant enrichment of plasma phytosterol concentrations, we are confident that our G5G8<sup>-/-</sup> mouse model does not have functional G5G8 protein as had been earlier shown by Yu et al. (7, 24), who originally generated this line of mice.

We assessed the functionality of ACAT2 in the jejunum by measuring enzyme activity with microsomal ACAT assays. The relative ACAT2 versus ACAT1 enzyme activities

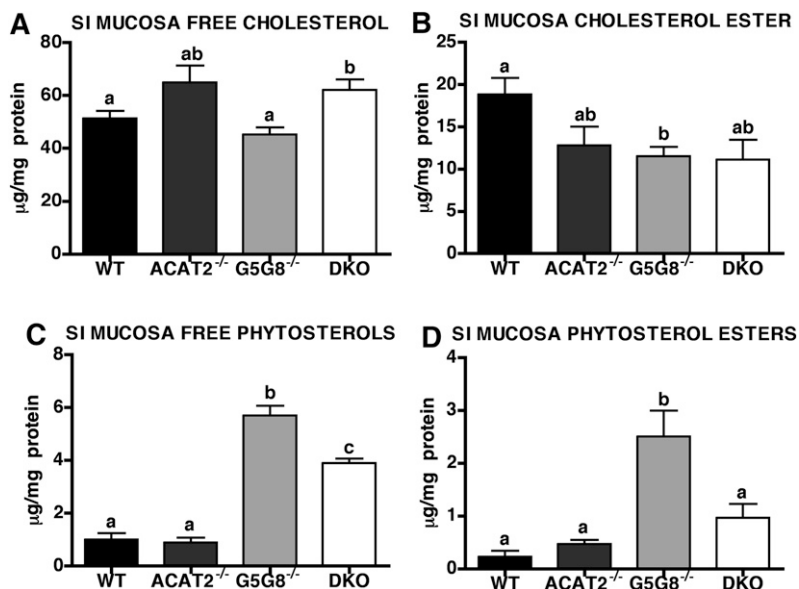


**Fig. 3.** Sterol concentrations in the mucosa of small intestine jejunum. Mice were fasted for 4 h prior to euthanasia. The small intestine was flushed clean with saline and divided into five equidistant sections. The mucosa of the second and third segments was gently scraped with glass slides and extracted with chloroform:methanol (2:1). The total lipid extract was subjected to GC analyses for (A) free cholesterol, (B) cholesterol ester, (C) free phytosterols, and (D) phytosterol esters. All values were normalized by protein concentration in the same sample. The data represent mean  $\pm$  SEM, n = 8–10/genotype. Unlike letters denote statistically significant differences ( $P < 0.05$ ) as determined by one-way ANOVA analyses and Tukey posthoc tests.



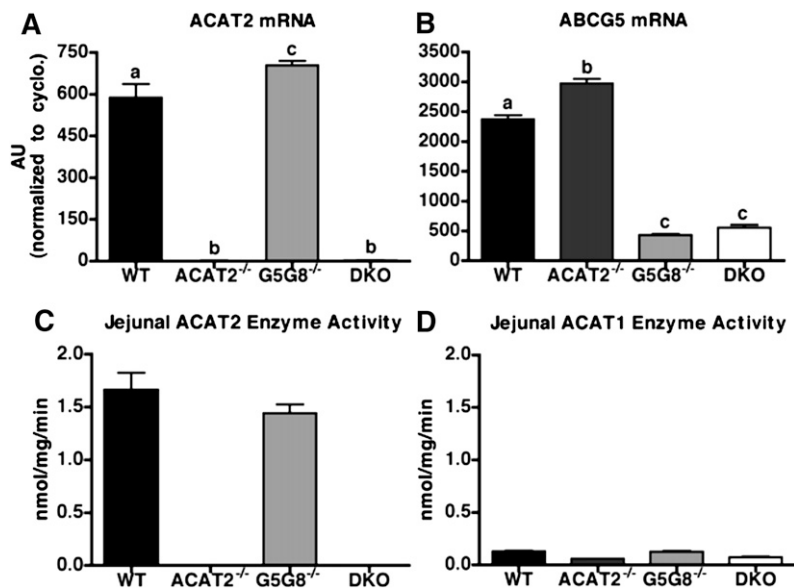


**Fig. 4.** ACAT2 and ABCG5 mRNA expression and ACAT enzyme activity in the jejunum. Real-time PCR analyses were done on SI-2 and SI-3, combined, to quantify relative gene expressions for ACAT2 (A) and ABCG5 (B) in the jejunum. The data are presented as arbitrary units (AU) normalized to cyclophilin gene expression. (C and D) In vitro ACAT assays were performed on microsomes isolated from the jejunum of mice. Pyripropene A, an ACAT2-specific inhibitor, was added to assess ACAT1 enzyme activity (D) in each sample, and ACAT2 enzyme activity (C) was calculated by subtracting values of ACAT1 activity from the total ACAT activity in each sample. The data represent mean  $\pm$  SEM,  $n = 5$ /genotype. Unlike letters indicate statistically significant differences ( $P < 0.05$ ) as determined by one-way ANOVA analyses and Tukey posthoc tests.

were measured (Fig. 4C, D). Despite having slightly elevated ACAT2 mRNA expression compared with WT mice (Fig. 4A), G5G8<sup>-/-</sup> mice had the same level of ACAT2 enzyme activity as WT mice (Fig. 4C). Neither ACAT2 mRNA (Fig. 4A) nor ACAT2 enzyme activity (Fig. 4C) was detectable in ACAT2-deficient mice. ACAT1 activity was minimal in all four genotypes, and the relative ACAT1 enzyme activity was not higher in the absence of ACAT2 (Fig. 4D). Thus, normally ACAT2 provides the majority of total ACAT enzyme activity in the SI.

As the newly absorbed sterols are transported in chylomicrons as sterol esters, we also measured the percentage of radioactivity distributed into free versus esterified sterols in isolated chylomicron particles. The results showed a major decrease in chylomicron [<sup>14</sup>C]CE when ACAT2 was deleted (Fig. 5B). WT chylomicrons possessed  $82.9 \pm 2.0\%$  of total [<sup>14</sup>C]cholesterol as CE (Fig. 5A), whereas G5G8<sup>-/-</sup> chylomicrons had significantly less [<sup>14</sup>C]cholesterol ( $70.2 \pm 4.7\%$ ) in the ester form (Fig. 5C). In contrast, about 85–88% of [<sup>14</sup>C]cholesterol was incorporated onto chylomicron particles in the unesterified form when ACAT2 enzyme activity was absent (Fig. 5B, D). Only 12–15% of the [<sup>14</sup>C]cholesterol in ACAT2<sup>-/-</sup> and DKO chylomicrons was found in the ester form. The source of this material is currently unidentified, and its identity as true cholesterol ester is not proven, but we suspect it was not derived from ACAT1, because ACAT1 enzyme activity is low in the SI (Fig. 4D) and ACAT1 protein is not expressed in the enterocyte (12).

Although ACAT2 efficiently esterified the majority of [<sup>14</sup>C]cholesterol in chylomicrons, the percentage of [<sup>3</sup>H]sitosterol esterification by ACAT2 was significantly lower. Only  $44.8 \pm 2.9\%$  and  $30.5 \pm 2.9\%$  of the [<sup>3</sup>H]sitosterol was esterified in WT and G5G8<sup>-/-</sup> chylomicrons, respectively (Fig. 5A, C). The majority of [<sup>3</sup>H]sitosterol in WT and G5G8<sup>-/-</sup> mice was packaged into chylomicrons in the unesterified (free) form. When ACAT2 was deleted, about 97% of the [<sup>3</sup>H]sitosterol remained unesterified (Fig. 5B, D).

Collectively, the data demonstrate that ACAT2 esterified significantly more [<sup>14</sup>C]cholesterol than [<sup>3</sup>H]sitosterol in chylomicrons regardless of presence or absence of G5G8 in the enterocyte and that less ACAT2 esterification occurred for both sterols when G5G8 was deleted.

The data on percentage radioactivity distribution into free sterols versus sterol esters (Fig. 5) was further supported by chylomicron sterol mass quantifications (Fig. 6), which expressed chylomicron particle mass composition [FC, CE, phospholipid (PL), triglyceride (TG), and protein] as cumulative mass ( $\mu\text{g}$ ) per hourly collection (mean  $\pm$  SEM) throughout the 8 h experiment. FP and PE data are not shown here, because they were not detected in WT or ACAT2<sup>-/-</sup> chylomicrons and constituted a negligible portion (0.13–0.25%) of the total chylomicron mass when G5G8 was deleted.

By the end of 8 h, ACAT2<sup>-/-</sup> mice produced chylomicrons with more cumulative FC mass ( $563 \pm 39 \mu\text{g}$ ) than WT mice ( $376 \pm 30 \mu\text{g}$ ), whereas G5G8<sup>-/-</sup> mice produced less chylomicron FC ( $213 \pm 7 \mu\text{g}$ ) (Fig. 6A). Despite this large reduction in FC mass secretion in G5G8<sup>-/-</sup> chylomicrons, the percentage of chylomicron particle composition as FC was comparable between WT ( $1.7 \pm 0.1\%$ ) and G5G8<sup>-/-</sup> ( $1.3 \pm 0.0\%$ ) chylomicrons (Table 1). No statistically significant difference was seen between cumulative FC masses from WT and DKO chylomicrons ( $363 \pm 98 \mu\text{g}$ ), which made up 3% or less of the total particle mass in these two genotypes.

The most contrasting data are shown in Fig. 6B. Cumulative secretion of CE mass was minimal when ACAT2 was deleted, totaling only  $25 \pm 11 \mu\text{g}$  and  $33 \pm 11 \mu\text{g}$  in ACAT2<sup>-/-</sup> and DKO chylomicrons, respectively, at 8 h. CE was secreted into chylomicrons of WT mice in an almost linear fashion, reaching  $2,089 \pm 238 \mu\text{g}$  CE after 8 h. By contrast, G5G8<sup>-/-</sup> mice secreted about 70% less CE mass ( $641 \pm 42 \mu\text{g}$  CE at 8 h) than WT mice (Fig. 6B), despite having comparable ACAT2 mRNA expression and enzyme activity as WT mice (Fig. 4A, C). In terms of percentage particle mass composition, CE made up  $10.0 \pm 1.0\%$  of the

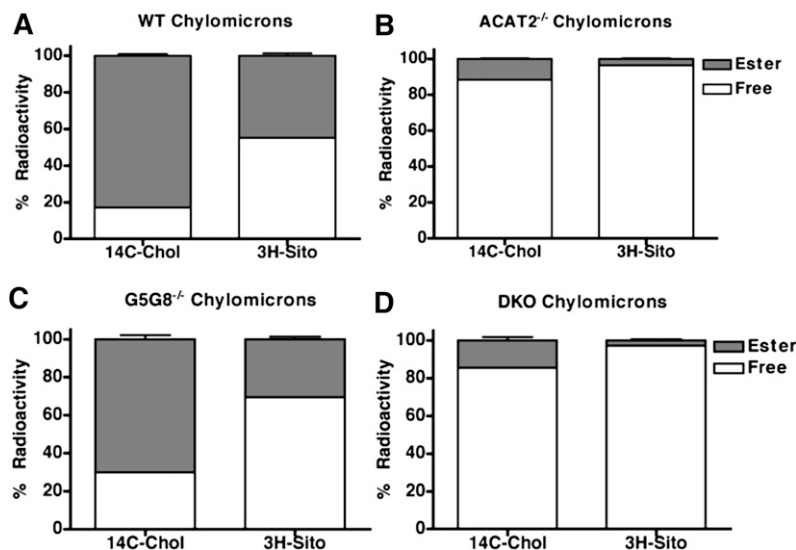


**Fig. 5.** Percentage radioactivity distribution into free sterols and sterol esters in isolated chylomicrons. Chylomicrons were isolated from lymph of wild-type (A), *ACAT2*<sup>-/-</sup> (B), *G5G8*<sup>-/-</sup> (C), and DKO (D) mice by ultracentrifugation, and the total lipid extracts were separated into free sterols and sterol esters by thin layer chromatography. [<sup>14</sup>C]cholesterol dpm and [<sup>3</sup>H]sitosterol dpm were measured in both sterol fractions, and the data are shown as percentages of total dpm distributed into free sterols and sterol esters. The data represent mean ± SEM, n = 5/genotype.

total particle mass in WT chylomicrons, but this value was decreased to only  $3.9 \pm 0.3\%$  in *G5G8*<sup>-/-</sup> chylomicrons (Table 1). Taken together, these results clearly demonstrate that chylomicron CE is mostly derived from ACAT2 and that *G5G8* deficiency reduces cholesterol availability for chylomicron transport, so that transport of both FC and CE (the latter through decreased cholesterol esterification by ACAT2) in *G5G8*<sup>-/-</sup> chylomicron particles was reduced (Fig. 6).

For chylomicrons of *ACAT2*<sup>-/-</sup> and DKO mice, the difference between the 12–15% radioactivity as CE (Fig. 5B, D) compared with the considerably lesser amount of CE mass transport (Fig. 6B) seemed to be more apparent than real. The chylomicron CE mass was measured by GLC as the difference between total cholesterol before and after saponification, whereas the material appearing as radioactive CE was separated by thin layer chromatography (TLC). The [<sup>14</sup>C]cholesterol tracer recovered in the CE position by TLC might not reflect true CE mass. In both cases, the esterification of cholesterol was significantly reduced in *ACAT2*-deficient mice. The majority of our data do not support the likelihood that real CE mass was as high as 12–15%. The enzymatic source of any ester that could have been formed by the intestine of *ACAT2*-deficient mice is unknown. It could be ACAT1, but this seems unlikely because ACAT1 has not been found in the enterocyte (12). It is possible that some of the wax esterases reported by Turkish et al. (36) made a contribution, but the mass of material present in this fraction was too low to identify the fatty acid profile.

In addition to lowering CE secretion, *G5G8* deficiency also appeared to reduce chylomicron PL, TG, and protein mass secretion as measured after 8 h (Fig. 6C, E). However, light scatter measurements showed that chylomicron particle size was similar (~145 nm in diameter) across all four genotypes (data not shown). Although the mass transport values for phospholipid, triglyceride, and protein appeared to be significantly lower in chylomicrons from *G5G8*<sup>-/-</sup> and DKO mice relative to WT mice, their percentages as part of the total particle composition remained

relatively consistent across all four genotypes, with 11.4–12.8% as PL, 71.6–80.6% as TG, and 4.9–6.0% as protein (Table 1). These data suggest that *G5G8*-deficient mice produced fewer numbers of chylomicron particles of relatively normal composition.

To further evaluate the possibility of abnormal chylomicron assembly in *G5G8*-deficient mice, we measured gene expression of microsomal transfer protein (MTP) and apolipoprotein B (apoB) but found no downregulation of either gene (supplemental Table I). Further, there was no indication of ER stress, evidenced by the fact that we found no perturbation in gene expressions of various ER-stress markers, such as X-box binding protein 1 (Xbp-1), X-box binding protein 1 spliced variant (Xbp-1p), activating transcription factor 6 (Atf-6), and DNA damage-inducible transcript 3 (Ddit-3), in the jejunum of *G5G8*<sup>-/-</sup> mice compared with other genotype groups. These data, together with the similar size and compositions of the chylomicron particles from all genotypes, suggest that the *G5G8*-deficient mice made normal but fewer chylomicron particles. The reason(s) for this outcome remain unknown.

## DISCUSSION

In previous studies on *ABCG5* and/or *ABCG8* (37, 38), fecal sterol excretion data suggested that *G5G8* functions as an inside-out sterol transporter because *G5G8* deficiency decreased sterol excretion and *G5G8* overexpression increased sterol excretion. However, the decrease in fecal sterol excretion could be a result of reduced sterol secretion into bile when *G5G8* is deleted. In this study, we investigated how *G5G8* deficiency affects sterol absorption efficiency, with a focus on cholesterol metabolism and chylomicron transport using the TLDC technique. The absence of *G5G8* resulted in a statistically significant 21% decrease in cholesterol absorption efficiency in *G5G8*<sup>-/-</sup> mice relative to WT mice (Fig. 1A, B). This decrease in percentage cholesterol absorption was associated with reductions in CE accumulation in the SI mucosa (Fig. 3B), in the percentage of chylomicron [<sup>14</sup>C]CE (Fig. 5C), in



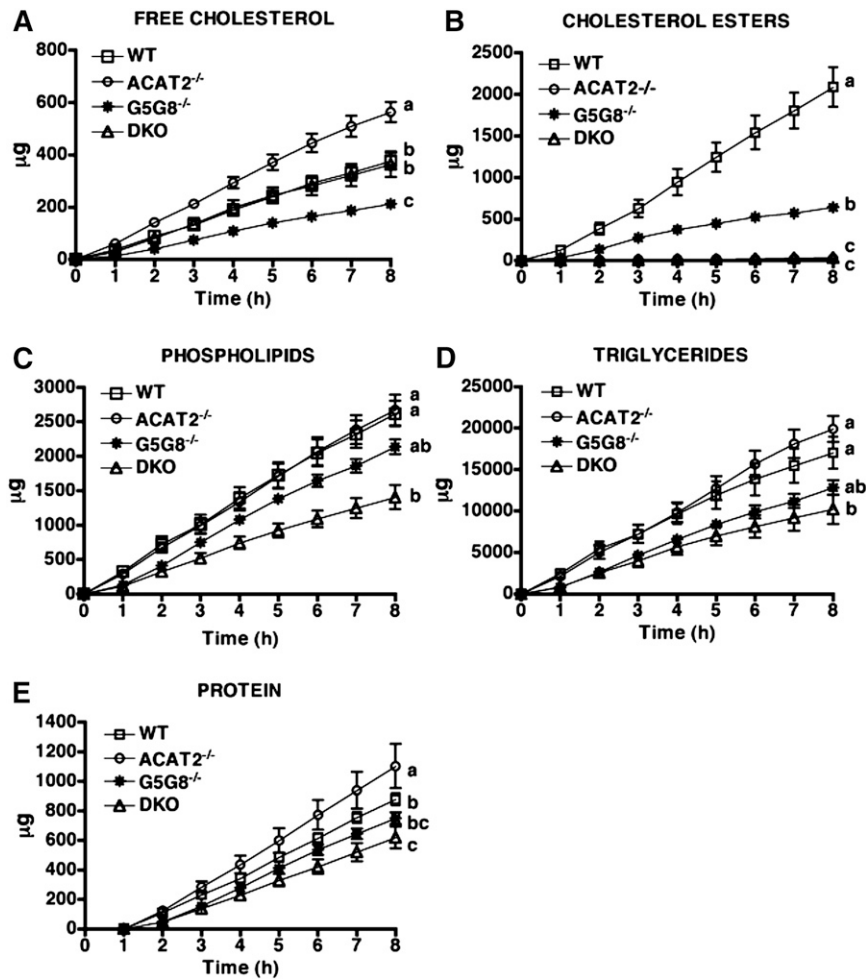


**Fig. 6.** Chylomicron particle mass composition throughout 8 h of lymph collection. Chylomicrons were isolated from lymph of WT, ACAT2<sup>-/-</sup>, G5G8<sup>-/-</sup>, and DKO mice by ultracentrifugation. After Bligh-Dyer extraction, free cholesterol (A) and cholesterol ester (B) masses were quantified by gas chromatography. Phospholipid mass (C) was measured by inorganic phosphorous colorimetric assay. Triglyceride mass (D) was measured by an enzymatic triglyceride kit from Wako as instructed by the manufacturer. Protein mass (E) was measured by a modified Lowry assay. The data show the average cumulative mass ( $\pm$  SEM,  $n = 5$ /genotype) of free cholesterol, cholesterol esters, phospholipids, triglycerides, and protein throughout the 8 h experiment. The data were analyzed by two-way ANOVA with Bonferroni posthoc tests. Unlike letters designate statistically significant differences of  $P < 0.05$  at the hour 8 time point.

cumulative CE mass secretion into chylomicrons (Fig. 6B), and in the percentage of total chylomicron particle mass as CE (Table 1). Altogether, the data strongly suggest that cholesterol esterification in the enterocyte, primarily from the activity of ACAT2, was dampened in the absence of G5G8. The intestine also appeared to exhibit differential handling of [<sup>14</sup>C]cholesterol versus [<sup>3</sup>H]sitosterol along the length of the GI tract (Fig. 2). In addition, the pattern of CE accumulation in the SI mucosa (Fig. 3B) was different compared with that in the liver (supplemental Fig. II-B), suggesting that G5G8 exerts different effects on cholesterol metabolism in the two tissues.

Data in the current study also differed from other reports in the literature, which used the fecal dual-isotope method to estimate fractional cholesterol absorption in mice with altered G5G8 expression (14, 24). This indirect method involves using a single oral dose of labeled cholesterol and a nonabsorbable reference marker, such as

$\beta$ -sitosterol or sitostanol. It measures the ratio of the radioactive labels in the starting mixture and in feces and assumes that there will be negligible absorption of the sitosterol tracers. However, in mice with altered sitosterol absorption, such as G5G8-deficient mice, sitosterol is not a nonabsorbable marker. These mice absorbed 3-fold more [<sup>3</sup>H]sitosterol than mice with intact G5G8 (Fig. 1D, E).

Our original hypothesis was that sterols enter the enterocyte through the brush border membrane via an NPC1L1-mediated process, with G5G8 subsequently limiting substrate availability for ACAT2-mediated sterol esterification by transporting unesterified cholesterol and phytosterols back out of the cell before ACAT2 esterification can occur, in the process decreasing the absorption efficiency of both sterols. To some extent, our results supported this hypothesis for phytosterols but not for cholesterol.

Although there was no surprise that the lack of sterol esterification in ACAT2<sup>-/-</sup> mice would reduce cholesterol

TABLE 1. Percentage composition of chylomicron particle mass

	% Particle Mass					
	Protein	PL	FC	TG	CE	Surface to Core
WT	4.9 ± 0.3 <sup>a</sup>	11.8 ± 0.3 <sup>a</sup>	1.7 ± 0.1 <sup>a</sup>	71.6 ± 1.7 <sup>a</sup>	10.0 ± 1.0 <sup>a</sup>	0.225
ACAT2 <sup>-/-</sup>	5.6 ± 0.2 <sup>a,b</sup>	11.4 ± 0.3 <sup>b</sup>	2.4 ± 0.1 <sup>a,b</sup>	80.6 ± 0.5 <sup>b</sup>	0.1 ± 0.0 <sup>b</sup>	0.240
G5G8 <sup>-/-</sup>	5.3 ± 0.3 <sup>a</sup>	12.8 ± 0.2 <sup>c</sup>	1.3 ± 0.0 <sup>a</sup>	76.5 ± 0.3 <sup>c</sup>	3.9 ± 0.3 <sup>c</sup>	0.243
DKO	6.0 ± 0.5 <sup>b</sup>	11.5 ± 0.2 <sup>a,b</sup>	3.0 ± 0.1 <sup>b</sup>	78.8 ± 0.7 <sup>b</sup>	0.3 ± 0.1 <sup>b</sup>	0.260

Mass ( $\mu\text{g}$ ) of protein, phospholipids (PL), free cholesterol (FC), triglycerides (TG) and cholesterol esters (CE) was measured in chylomicrons isolated from eight hourly collections for each animal. The percentage composition was calculated by dividing each component mass by the sum of all masses for each chylomicron sample from each time point. The mean percentages of all eight time points from one individual animal were calculated for each particle component. The data were expressed the overall mean  $\pm$  SEM for each genotype ( $n = 5/\text{genotype}$ ). The surface-to-core ratio was calculated by dividing the sum of protein, PL, and FC by the sum of TG and CE.

<sup>a,b,c</sup>Unlike letters denote statically significant difference ( $P < 0.05$ ) within the same column as measured by one-way ANOVA and Tukey posthoc tests.

absorption efficiency, we were surprised to observe a decrease in percentage cholesterol absorption when G5G8 was deleted (Fig. 1A, B). On the basis of previous publications (37, 39) and the indirect finding that G5G8<sup>-/-</sup> mice displayed decreased fecal cholesterol excretion (Fig. 1C), we anticipated that G5G8 disruption would be associated with more efficient cholesterol absorption. However, this result was not seen when TLDC was performed to directly measure percentage cholesterol absorption. G5G8<sup>-/-</sup> mice had a statistically significant 21% reduction in cholesterol absorption efficiency. A combination of factors may have led to this outcome. In the absence of G5G8, there was some phytosterol accumulation in SI mucosa (Fig. 3C, D). It is possible that the enrichment of phytosterols in the cell membrane may have led to NPC1L1 dysfunction, thus reducing cholesterol uptake into the enterocyte (40–43). Ge et al. (44, 45) and Zhang et al. (46) have shown that NPC1L1-mediated cholesterol uptake at the plasma membrane involves lipid raft proteins, flotillins, and that NPC1L1 flotillin-containing cholesterol-enriched membrane microdomains are internalized into the cell via a clathrin-coated pit pathway. These researchers found that NPC1L1 selectively binds cholesterol but not phytosterols, and more particularly they found that phytosterols do not bind the NPC1L1 N-terminal domain or induce NPC1L1 endocytosis. The incorporation of phytosterols into a phospholipid membrane has also been shown to weaken the stability of the membrane (47). Taken together, a possible consequence may be reduced cholesterol availability for ACAT2 esterification, as evidenced by the reduction in percentage [<sup>14</sup>C]cholesterol as esterified sterols (Fig. 5) and the decrease in chylomicron CE mass secretion (Fig. 6B). Furthermore, a possible reduction in cholesterol uptake, resulting from phytosterol membrane enrichment, may have triggered upregulation of NPC1L1 mRNA expression in G5G8<sup>-/-</sup> jejunum (supplemental Table I), in effect changing the capacity to handle increased cholesterol uptake into the enterocyte (46).

Interestingly, there was obvious differential handling of [<sup>14</sup>C]cholesterol and [<sup>3</sup>H]sitosterol throughout the length of GI tract (Fig. 2). Very little [<sup>3</sup>H]sitosterol was present the SI wall, even in the absence of G5G8. If NPC1L1 had facilitated efficient uptake of both cholesterol and phytosterols as previously suggested (14), one would suspect that


higher amounts of [<sup>3</sup>H]sitosterol would have accumulated in the gut wall of mice, particularly when G5G8 was not available to act as the sterol excretion pump. Instead, no appreciable amount of [<sup>3</sup>H]sitosterol was detected in the proximal SI. Most of the [<sup>3</sup>H]sitosterol was found in the distal GI tract, and the amount of [<sup>3</sup>H]sitosterol detected distally was similar among all four genotypes. By contrast, [<sup>14</sup>C]cholesterol was well incorporated throughout the proximal SI, and the levels found in G5G8-deficient mice did not exceed those found in mice lacking ACAT2. Altogether, the data demonstrate that phytosterols are not efficiently taken up into the gut wall, regardless of the presence or absence of G5G8. These results indicate that the primary discriminators between cholesterol and phytosterol absorption may be present at the levels of NPC1L1-mediated sterol uptake and ACAT2 sterol esterification, not necessarily at G5G8-mediated sterol excretion. Perhaps in alignment with recent findings of in vitro studies (42, 44, 46, 48), NPC1L1 is the initial gatekeeper that facilitates cholesterol uptake into the enterocyte, while at the same time limiting phytosterol uptake. To the extent that this system could be potentially leaky, G5G8 may serve as a secondary “clean-up” mechanism for removing the phytosterol molecules that make it past NPC1L1. When this “clean-up” mechanism is lost with G5G8 disruption, then even the small 6–7% of phytosterol absorption in sitosterolemic mice (Fig. 1D, E) and humans (1) can lead to significantly more accumulation of phytosterols over time. The assumption is that without G5G8, phytosterols cannot be efficiently excreted from the enterocytes of the SI or the hepatocytes of the liver.

We hypothesize that the preference for absorbing cholesterol, but not phytosterols, involves a multistep process. Our data support the notion that NPC1L1 at the brush border membrane discriminates against phytosterols and allows predominantly cholesterol into the enterocyte. Any phytosterols that escaped the primary screening by NPC1L1 may then be shuttled out of the cell by a secondary pathway involving G5G8. The remaining sterols from NPC1L1 uptake (mostly cholesterol and some phytosterols) enter the putative substrate pool for ACAT2 by either vesicular or nonvesicular transport (48–51). In the ER, ACAT2 adds another layer of selectivity by preferentially esterifying cholesterol rather than phytosterols. When

G5G8 is functional, any nonesterified phytosterol molecule that gets returned to the plasma membrane can be excreted via G5G8. Without G5G8, the residual phytosterols remain in the cell and can make their way into the substrate pool for ACAT2. Once a sterol molecule is esterified by ACAT2, its physiochemical state favors incorporation into the neutral lipid core of a chylomicron particle, facilitating entry into the lymphatic system. Without ACAT2, significantly less sterol mass can be transported into lymph, because unesterified sterols only coat the surface of chylomicrons, limiting the abundance of cholesterol in these particles. Thus, ACAT2 esterification is necessary for efficient sterol absorption.

All chylomicrons must pool into the cisterna chyli, travel up the thoracic lymph duct, and enter the blood before arriving at the liver for final catabolism. Although murine livers express G5G8 but not NPC1L1, human livers express appreciable amounts of both (52, 53), which can again function as another layer of protection against any toxicity of phytosterols. The data show that the G5G8<sup>-/-</sup> livers accumulated phytosterols in both the free and ester forms, whereas livers of mice with intact G5G8 had almost undetectable concentrations of these sterols (supplemental Fig. II-C, D). In vitro data from hepatoma cells also suggest that NPC1L1 can preferentially transport unesterified cholesterol over sitosterol into the cell (40, 42). A publication on the structure of the N-terminal domain of NPC1L1 and its biochemical properties revealed a closed cholesterol binding pocket that possessed high selectivity for binding cholesterol but not sitosterol, because the ethyl group at carbon 24 on sitosterol would presumably cause an unfavorable steric hinderance (54). These researchers also found that sitosterol was not able to compete with cholesterol for binding to NPC1L1. On the basis of the published data, we believe that in the liver G5G8 excretes both cholesterol and phytosterols from the hepatocytes into bile, and then NPC1L1 selectively reabsorbs primarily cholesterol back into the hepatocytes. Once inside the cells, the sterols travel to the putative substrate pool for ACAT2, which then preferentially esterifies cholesterol instead of phytosterols (23).

Our study demonstrates that similar mechanisms of complex sterol selectivity may also exist in the enterocytes of the intestine. Together, NPC1L1, G5G8, and ACAT2 apparently orchestrate the first line of defense against dietary phytosterol absorption, in effect preferentially allowing cholesterol to enter the circulation via chylomicron transport through the lymphatic system. Admittedly, there is currently no direct evidence for a protein-protein interaction between NPC1L1 and G5G8 in the regulation of sterol influx-efflux pathways, but such a possibility seems consistent with the available data. It would be interesting to investigate whether NPC1L1 and G5G8 can physically interact with one another in the same membrane and/or intracellular compartment, and perhaps also with ACAT2, to efficiently determine membrane sterol composition and substrate availability for ACAT2 esterification. These ideas are only preliminary, and significantly more work is necessary to further establish the roles of these crucial

players in the enterocytes as well as in hepatocytes. The data generated from this study is merely a preliminary glimpse into the complex but fascinating black box of intestinal sterol absorption. 

The authors thank Dr. Martha Wilson, Mr. Ramesh Shah, and Dr. Thomas Smith of Wake Forest University Health Sciences as well as Dr. Paolo Parini of the Karolinska Institute for their technical expertise and guidance.

## REFERENCES

- Bhattacharyya, A. K., and W. E. Connor. 1974. Beta-sitosterolemia and xanthomatosis. A newly described lipid storage disease in two sisters. *J. Clin. Invest.* **53**: 1033–1043.
- Normén, A. L., H. A. Brants, L. E. Voorrips, H. A. Andersson, P. A. van den Brandt, and R. A. Goldbohm. 2001. Plant sterol intakes and colorectal cancer risk in the Netherlands Cohort Study on Diet and Cancer. *Am. J. Clin. Nutr.* **74**: 141–148.
- Weihrauch, J. L., and J. M. Gardner. 1978. Sterol content of foods of plant origin. *J. Am. Diet. Assoc.* **73**: 39–47.
- Kidambi, S., and S. B. Patel. 2008. Sitosterolaemia: pathophysiology, clinical presentation and laboratory diagnosis. *J. Clin. Pathol.* **61**: 588–594.
- Bosner, M. S., L. G. Lange, W. F. Stenson, and R. E. Ostlund, Jr. 1999. Percent cholesterol absorption in normal women and men quantified with dual stable isotopic tracers and negative ion mass spectrometry. *J. Lipid Res.* **40**: 302–308.
- Von Bergmann, K., D. Lutjohann, B. Lindenthal, and A. Steinmetz. 2003. Efficiency of intestinal cholesterol absorption in humans is not related to apoE phenotype. *J. Lipid Res.* **44**: 193–197.
- Yu, L., K. von Bergmann, D. Lutjohann, H. H. Hobbs, and J. C. Cohen. 2004. Selective sterol accumulation in ABCG5/ABCG8-deficient mice. *J. Lipid Res.* **45**: 301–307.
- Salen, G., I. Horak, M. Rothkopf, J. L. Cohen, J. Speck, G. S. Tint, V. Shore, B. Dayal, T. Chen, and S. Shefer. 1985. Lethal atherosclerosis associated with abnormal plasma and tissue sterol composition in sitosterolemia with xanthomatosis. *J. Lipid Res.* **26**: 1126–1133.
- Salen, G., V. Shore, G. S. Tint, T. Forte, S. Shefer, I. Horak, E. Horak, B. Dayal, L. Nguyen, A. K. Batta, et al. 1989. Increased sitosterol absorption, decreased removal, and expanded body pools compensate for reduced cholesterol synthesis in sitosterolemia with xanthomatosis. *J. Lipid Res.* **30**: 1319–1330.
- Graf, G. A., W. P. Li, R. D. Gerard, I. Gelissen, A. White, J. C. Cohen, and H. H. Hobbs. 2002. Coexpression of ATP-binding cassette proteins ABCG5 and ABCG8 permits their transport to the apical surface. *J. Clin. Invest.* **110**: 659–669.
- Repa, J. J., K. E. Berge, C. Pomajzl, J. A. Richardson, H. Hobbs, and D. J. Mangelsdorf. 2002. Regulation of ATP-binding cassette sterol transporters ABCG5 and ABCG8 by the liver X receptors alpha and beta. *J. Biol. Chem.* **277**: 18793–18800.
- Lee, R. G., M. C. Willingham, M. A. Davis, K. A. Skinner, and L. L. Rudel. 2000. Differential expression of ACAT1 and ACAT2 among cells within liver, intestine, kidney, and adrenal of nonhuman primates. *J. Lipid Res.* **41**: 1991–2001.
- Tang, W., Y. Ma, L. Jia, Y. A. Ioannou, J. P. Davies, and L. Yu. 2009. Genetic inactivation of NPC1L1 protects against sitosterolemia in mice lacking ABCG5/ABCG8. *J. Lipid Res.* **50**: 293–300.
- Lütjohann, D., I. Björkhem, U. F. Beil, and K. von Bergmann. 1995. Sterol absorption and sterol balance in phytosterolemia evaluated by deuterium-labeled sterols: effect of sitostanol treatment. *J. Lipid Res.* **36**: 1763–1773.
- Mueller, J. H. 1916. The mechanism of cholesterol absorption. *J. Biol. Chem.* **27**: 463–480.
- Klein, R. L., and L. L. Rudel. 1983. Cholesterol absorption and transport in thoracic duct lymph lipoproteins of nonhuman primates. Effect of dietary cholesterol level. *J. Lipid Res.* **24**: 343–356.
- Vahouny, G. V., and C. R. Treadwell. 1957. Changes in lipid composition of lymph during cholesterol absorption in the rat. *Am. J. Physiol.* **191**: 179–184.
- Linder, E., and R. Blomstrand. 1958. Technic for collection of thoracic duct lymph of man. *Proc. Soc. Exp. Biol. Med.* **97**: 653–657.



19. Rudel, L. L., J. M. Felts, and M. D. Morris. 1973. Exogenous cholesterol transport in rabbit plasma lipoproteins. *Biochem. J.* **134**: 531–537.
20. Buhman, K. K., M. Accad, S. Novak, R. S. Choi, J. S. Wong, R. L. Hamilton, S. Turley, and R. V. Farese, Jr. 2000. Resistance to diet-induced hypercholesterolemia and gallstone formation in ACAT2-deficient mice. *Nat. Med.* **6**: 1341–1347.
21. Field, F. J., E. Born, and S. N. Mathur. 1997. Effect of micellar beta-sitosterol on cholesterol metabolism in CaCo-2 cells. *J. Lipid Res.* **38**: 348–360.
22. Field, F. J., and S. N. Mathur. 1983. beta-sitosterol: esterification by intestinal acylcoenzyme A: cholesterol acyltransferase (ACAT) and its effect on cholesterol esterification. *J. Lipid Res.* **24**: 409–417.
23. Temel, R. E., A. K. Gebre, J. S. Parks, and L. L. Rudel. 2003. Compared with Acyl-CoA:cholesterol O-acyltransferase (ACAT) 1 and lecithin:cholesterol acyltransferase, ACAT2 displays the greatest capacity to differentiate cholesterol from sitosterol. *J. Biol. Chem.* **278**: 47594–47601.
24. Yu, L., R. E. Hammer, J. Li-Hawkins, K. Von Bergmann, D. Lutjohann, J. C. Cohen, and H. H. Hobbs. 2002. Disruption of Abcg5 and Abcg8 in mice reveals their crucial role in biliary cholesterol secretion. *Proc. Natl. Acad. Sci. USA.* **99**: 16237–16242.
25. Temel, R. E., R. G. Lee, K. L. Kelley, M. A. Davis, R. Shah, J. K. Sawyer, M. D. Wilson, and L. L. Rudel. 2005. Intestinal cholesterol absorption is substantially reduced in mice deficient in both ABCA1 and ACAT2. *J. Lipid Res.* **46**: 2423–2431.
26. Ionac, M. 2003. One technique, two approaches, and results: thoracic duct cannulation in small laboratory animals. *Microsurgery.* **23**: 239–245.
27. Nguyen, T. M., J. K. Sawyer, K. L. Kelley, M. A. Davis, and L. L. Rudel. 2012. Cholesterol esterification by ACAT2 is essential for efficient intestinal cholesterol absorption: evidence from thoracic lymph duct cannulation. *J. Lipid Res.* **53**: 95–104.
28. Lee, R. G., R. Shah, J. K. Sawyer, R. L. Hamilton, J. S. Parks, and L. L. Rudel. 2005. ACAT2 contributes cholesteryl esters to newly secreted VLDL, whereas LCAT adds cholesteryl ester to LDL in mice. *J. Lipid Res.* **46**: 1205–1212.
29. Temel, R. E., L. Hou, L. L. Rudel, and G. S. Shelness. 2007. ACAT2 stimulates cholesteryl ester secretion in apoB-containing lipoproteins. *J. Lipid Res.* **48**: 1618–1627.
30. Bell 3rd, T. A., J. M. Brown, M. J. Graham, K. M. Lemonidis, R. M. Croke, and L. L. Rudel. 2006. Liver-specific inhibition of acyl-coenzyme a:cholesterol acyltransferase 2 with antisense oligonucleotides limits atherosclerosis development in apolipoprotein B100-only low-density lipoprotein receptor<sup>-/-</sup> mice. *Arterioscler. Thromb. Vasc. Biol.* **26**: 1814–1820.
31. Lowry, O. H., N. J. Rosebrough, A. L. Farr, and R. J. Randall. 1951. Protein measurement with the Folin phenol reagent. *J. Biol. Chem.* **193**: 265–275.
32. Yu, L., S. Gupta, F. Xu, A. D. Liverman, A. Moschetta, D. J. Mangelsdorf, J. J. Repa, H. H. Hobbs, and J. C. Cohen. 2005. Expression of ABCG5 and ABCG8 is required for regulation of biliary cholesterol secretion. *J. Biol. Chem.* **280**: 8742–8747.
33. Temel, R. E., J. K. Sawyer, L. Yu, C. Lord, C. Degirolamo, A. McDaniel, S. Marshall, N. Wang, R. Shah, L. L. Rudel, et al. 2010. Biliary sterol secretion is not required for macrophage reverse cholesterol transport. *Cell Metab.* **12**: 96–102.
34. Temel, R. E., T. Tang, T. Ma, L. L. Rudel, M. C. Willingham, Y. A. Ioannou, J. P. Davies, L. Nilsson, and L. Yu. 2007. Hepatic Niemann-Pick C1-Like 1 regulates biliary cholesterol concentration and is a target of ezetimibe. *J. Clin. Invest.* **117**: 1968–1978.
35. Turley, S. D., M. A. Valasek, J. J. Repa, and J. M. Dietschy. 2010. Multiple mechanisms limit the accumulation of unesterified cholesterol in the small intestine of mice deficient in both ACAT2 and ABCA1. *Am. J. Physiol. Gastrointest. Liver Physiol.* **299**: G1012–G1022.
36. Turkish, A. R., A. L. Henneberry, D. Cromley, M. Padamsee, P. Oelkers, H. Bazzi, A. M. Christiano, J. T. Billheimer, and S. L. Sturley. 2005. Identification of two novel human acyl-CoA wax alcohol acyltransferases. *J. Biol. Chem.* **280**: 14755–14764.
37. Yu, L., J. Li-Hawkins, R. E. Hammer, K. E. Berge, J. D. Horton, J. C. Cohen, and H. H. Hobbs. 2002. Overexpression of ABCG5 and ABCG8 promotes biliary cholesterol secretion and reduces fractional absorption of dietary cholesterol. *J. Clin. Invest.* **110**: 671–680.
38. Wang, H. H., S. B. Patel, M. C. Carey, and D. Q. Wang. 2007. Quantifying anomalous intestinal sterol uptake, lymphatic transport, and biliary secretion in Abcg8<sup>(-/-)</sup> mice. *Hepatology.* **45**: 998–1006.
39. Lee, M. H., K. Lu, and S. B. Patel. 2001. Genetic basis of sitosterolemia. *Curr. Opin. Lipidol.* **12**: 141–149.
40. Yu, L., S. Bharadwaj, J. M. Brown, Y. Ma, W. Du, M. A. Davis, P. Michaely, P. Liu, M. C. Willingham, and L. L. Rudel. 2006. Cholesterol-regulated translocation of NPC1L1 to the cell surface facilitates free cholesterol uptake. *J. Biol. Chem.* **281**: 6616–6624.
41. Iyer, S. P., X. Yao, J. H. Crona, L. M. Hoos, G. Tetzloff, H. R. Davis, Jr., M. P. Graziano, and S. W. Altmann. 2005. Characterization of the putative native and recombinant rat sterol transporter Niemann-Pick C1 Like 1 (NPC1L1) protein. *Biochim. Biophys. Acta.* **1722**: 282–292.
42. Brown, J. M., L. L. Rudel, and L. Yu. 2007. NPC1L1 (Niemann-Pick C1-like 1) mediates sterol-specific unidirectional transport of non-esterified cholesterol in McArdle-RH7777 hepatoma cells. *Biochem. J.* **406**: 273–283.
43. Petersen, N. H., N. J. Faergeman, L. Yu, and D. Wustner. 2008. Kinetic imaging of NPC1L1 and sterol trafficking between plasma membrane and recycling endosomes in hepatoma cells. *J. Lipid Res.* **49**: 2023–2037.
44. Ge, L., J. Wang, W. Qi, H. H. Miao, J. Cao, Y. X. Qu, B. L. Li, and B. L. Song. 2008. The cholesterol absorption inhibitor ezetimibe acts by blocking the sterol-induced internalization of NPC1L1. *Cell Metab.* **7**: 508–519.
45. Ge, L., W. Qi, L. J. Wang, H. H. Miao, Y. X. Qu, B. L. Li, and B. L. Song. 2011. Flotillins play an essential role in Niemann-Pick C1-like 1-mediated cholesterol uptake. *Proc. Natl. Acad. Sci. USA.* **108**: 551–556.
46. Zhang, J. H., L. Ge, W. Qi, L. Zhang, H. H. Miao, B. L. Li, M. Yang, and B. L. Song. 2011. The N-terminal domain of NPC1L1 protein binds cholesterol and plays essential roles in cholesterol uptake. *J. Biol. Chem.* **286**: 25088–25097.
47. Hac-Wydro, K., P. Wydro, A. Jagoda, and J. Kapusta. 2007. The study on the interaction between phytosterols and phospholipids in model membranes. *Chem. Phys. Lipids.* **150**: 22–34.
48. Mesmin, B., and F. R. Maxfield. 2009. Intracellular sterol dynamics. *Biochim. Biophys. Acta.* **1791**: 636–645.
49. Maxfield, F. R., and D. Wustner. 2002. Intracellular cholesterol transport. *J. Clin. Invest.* **110**: 891–898.
50. Ikonen, E. 2008. Cellular cholesterol trafficking and compartmentalization. *Nat. Rev. Mol. Cell Biol.* **9**: 125–138.
51. Chang, T. Y., C. C. Chang, N. Ohgami, and Y. Yamauchi. 2006. Cholesterol sensing, trafficking, and esterification. *Annu. Rev. Cell Dev. Biol.* **22**: 129–157.
52. Pramfalk, C., Z. Y. Jiang, and P. Parini. 2011. Hepatic Niemann-Pick C1-like 1. *Curr. Opin. Lipidol.* **22**: 225–230.
53. Kidambi, S., and S. B. Patel. 2008. Cholesterol and non-cholesterol sterol transporters: ABCG5, ABCG8 and NPC1L1: a review. *Xenobiotica.* **38**: 1119–1139.
54. Kwon, H. J., M. Palnitkar, and J. Deisenhofer. 2011. The structure of the NPC1L1 N-terminal domain in a closed conformation. *PLoS ONE.* **6**: e18722.